

C: Energy Conversion and Storage; Energy and Charge Transport

Vibrational Effects in X-ray Absorption Spectra of 2D Layered MaterialsWeine Olovsson, Teruyasu Mizoguchi, Martin Magnuson,
Stefan Kontur, Olle Hellman, Isao Tanaka, and Claudia Draxl*J. Phys. Chem. C*, **Just Accepted Manuscript** • DOI: 10.1021/acs.jpcc.9b00179 • Publication Date (Web): 15 Feb 2019Downloaded from <http://pubs.acs.org> on February 15, 2019**Just Accepted**

“Just Accepted” manuscripts have been peer-reviewed and accepted for publication. They are posted online prior to technical editing, formatting for publication and author proofing. The American Chemical Society provides “Just Accepted” as a service to the research community to expedite the dissemination of scientific material as soon as possible after acceptance. “Just Accepted” manuscripts appear in full in PDF format accompanied by an HTML abstract. “Just Accepted” manuscripts have been fully peer reviewed, but should not be considered the official version of record. They are citable by the Digital Object Identifier (DOI®). “Just Accepted” is an optional service offered to authors. Therefore, the “Just Accepted” Web site may not include all articles that will be published in the journal. After a manuscript is technically edited and formatted, it will be removed from the “Just Accepted” Web site and published as an ASAP article. Note that technical editing may introduce minor changes to the manuscript text and/or graphics which could affect content, and all legal disclaimers and ethical guidelines that apply to the journal pertain. ACS cannot be held responsible for errors or consequences arising from the use of information contained in these “Just Accepted” manuscripts.



ACS Publications

is published by the American Chemical Society, 1155 Sixteenth Street N.W.,
Washington, DC 20036Published by American Chemical Society. Copyright © American Chemical Society.
However, no copyright claim is made to original U.S. Government works, or works
produced by employees of any Commonwealth realm Crown government in the course
of their duties.

Vibrational Effects in X-ray Absorption Spectra of 2D Layered Materials

Weine Olovsson,^{*,†} Teruyasu Mizoguchi,[‡] Martin Magnuson,[†] Stefan Kontur,[¶]
Olle Hellman,^{§,||} Isao Tanaka,[⊥] and Claudia Draxl^{¶,#}

[†]*Theoretical Physics, Department of Physics, Chemistry and Biology (IFM), Linköping
University, SE-581 83 Linköping, Sweden*

[‡]*Institute of Industrial Science, The University of Tokyo, Japan*

[¶]*Physics Department and IRIS Adlershof, Humboldt-Universität zu Berlin, Germany*

[§]*Department of Physics, Boston College, Chestnut Hill, Massachusetts 02467, USA*

^{||}*Department of Applied Physics and Materials Science, California Institute of Technology,
Pasadena, California 91125, USA*

[⊥]*Department of Materials Science and Engineering, Kyoto University, Sakyo, Japan*

[#]*European Theoretical Spectroscopy Facility (ETSF)*

E-mail: weine.olvsson@liu.se

Abstract

With the examples of the C K -edge in graphite and the B K -edge in hexagonal BN, we demonstrate the impact of vibrational coupling and lattice distortions on the X-ray absorption near-edge structure (XANES) in 2D layered materials. Theoretical XANES spectra are obtained by solving the Bethe-Salpeter equation of many-body perturbation theory, including excitonic effects through the correlated motion of core-hole and excited electron. We show that accounting for zero-point motion is important for the interpretation and understanding of the measured X-ray absorption fine structure in both materials, in particular for describing the σ^* -peak structure.

Introduction

X-ray absorption near-edge structure (XANES) is a powerful technique for the characterization of materials. It is used to identify chemical environment and bonding of specific elements by monitoring the electronic transitions between core levels and unoccupied states. Likewise, electron energy-loss near-edge structure (ELNES) by transmission electron microscopy can provide almost identical information. To fully utilize this spectral information, a reliable theoretical analysis can provide the required insight into the nature of the observed excitations.

There is a long history of computing core-level spectra from first principles. The majority of calculations¹ is based on density-functional theory (DFT)² utilizing the concept of a *core hole* in a supercell, also called the final-state approximation.^{3,4} Although this method has been successful in describing most of the spectral features, it turned out that sharp excitonic peaks appearing near the absorption edge, or intensity ratios, cannot be reproduced reliably. In such cases, one needs to go beyond the core-hole approximation and treat electron-hole interaction by solving the Bethe-Salpeter equation (BSE) of many-body perturbation theory.⁵⁻⁷ In this work, we demonstrate with the examples of graphite and hexagonal boron nitride, that another important step beyond this methodology is required to understand the

1
2
3 spectra of these layered systems.
4

5 Graphite and hexagonal boron nitride are archetypical 2D materials that have been in-
6 tensively discussed in the literature. However, neither the carbon K -edge ($1s$) spectra in
7 graphite nor that of boron in h -BN has been satisfactorily explained by *ab initio* theory. Due
8 to their hexagonal layered structures their excitation spectra are characterized by in-plane
9 and out-of-plane components. Both show a pronounced π^* -peak at the core edge, that stem
10 from p_z orbitals pointing in the direction perpendicular to the layers. The contribution of
11 the in-plane sp^2 orbitals is recognized as the main origin of the σ^* -peak structure, located
12 at roughly 6 eV above the π^* core-edge. Detailed experimental investigations revealed that
13 the σ^* -peak in both crystals exhibits a double-peak structure, labeled σ_1^* and σ_2^* .^{8,9}
14
15
16
17
18
19
20
21
22

23 The C K -edge absorption spectra in graphite has been calculated by various theoretical
24 methods, including a BSE scheme based on the pseudopotential approximation,¹⁰ a core-
25 hole supercell method^{11,12} and the Mahan-Nozières-De Dominices (MND) method.¹³ None
26 of them could resolve the double-peak structure. Similar double σ^* peaks are observed in the
27 boron K -edge of h -BN in XANES as well as ELNES experiments.⁹ Like for graphite, previous
28 DFT calculations did not obtain this striking feature.¹⁴ On the other hand, pseudopotential-
29 based BSE calculations¹⁵ showed the presence of a "camel-back", however its origin was not
30 clarified. In this work, we show that vibrational effects must be accounted for in order to
31 understand the shape of the σ^* region.
32
33
34
35
36
37
38
39
40

41 The impact of phonons and temperature effects on electronic excitations is an emerging
42 issue, however, there is no commonly accepted way of describing them from first princi-
43 ples. For example, the influence of symmetry-breaking effects from phonons or Jahn-Teller
44 distortions, has been discussed in the literature for graphite and other materials.^{8,16–22} In-
45 corporating electron-phonon coupling into the Bethe-Salpeter equation,²³ the temperature-
46 dependent optical spectra of silicon and h -BN were investigated. An alternative approach
47 based on stochastic modeling based on the Williams-Lax theory was used to account for
48 zero-point motions in the optical spectra of nano-diamonds.²⁴ More recent examples of core
49
50
51
52
53
54
55
56
57
58
59
60

excitations concern the Mg K -edge in MgO,²⁵ and N K -edge in h -BN.²⁶ Here, we approach the problem from two sides. First, we probe the sensitivity of the spectra to symmetry-breaking vibrational modes. Second, we apply an efficient statistical model^{27,28} to include the effect of electron-vibrational coupling on the near-edge structure.

Methodology

To obtain the X-ray absorption spectra, we solve the Bethe-Salpeter equation, using the open source code **exciting**,^{29,30} that has been successfully applied to K -edge excitations in other materials.³¹ For a detailed description of the implementation, see Ref.³⁰ and references therein. Being based on the all-electron full-potential linearized augmented plane-wave (FPLAPW) method, **exciting** gives access to the core region without further approximations than those inherent of the underlying exchange-correlation functional used for the DFT ground-state calculation. The latter is the generalized gradient approximation (GGA) in the PBE³² approach in our case. For both systems, experimental lattice constants are adopted.

First, we consider a computationally efficient approach which can be used to explore the general effect of lattice distortions on the spectra. Namely, we limit our study to phonon modes at the Γ point. For the E_{2g} modes, the unit cells consist of four atoms in two planes. For graphite, we use an $11 \times 11 \times 3$ \mathbf{k} -mesh and include 13 states above the Fermi-level in the setup of the BSE Hamiltonian for the distorted systems. For h -BN a $9 \times 9 \times 3$ \mathbf{k} -mesh and 25 unoccupied states were sufficient to capture the absorption fine structure.

Secondly, in order to probe the overall effect of lattice vibrations on the excitation spectra, we use an efficient stochastic sampling approach, see Refs.^{27,28} and references therein. We generate a set of structures to sample a canonical ensemble, averaging over the amplitude of each phonon mode:

$$\langle A_{is} \rangle = \sqrt{\frac{\hbar(2n_s + 1)}{2m_i\omega_s}}. \quad (1)$$

Given these amplitudes, supercells were constructed with the atomic positions given by

$$u_i = \sum_s Q_{is} \langle A_{is} \rangle \sqrt{-2 \ln \xi_1} \sin 2\pi \xi_2, \quad (2)$$

where, $0 < \xi < 1$ are uniform random numbers, ω the frequency, and Q the eigenvector of mode s . The temperature enters via the Bose occupation factor n_s . Here, the supercells consist of 16 atoms placed in two planes. Fifty structures were used for the sampling of graphite and 100 structures for h -BN. For graphite, we use a $4 \times 4 \times 1$ \mathbf{k} -mesh and include 50 states above the Fermi-level in the setup of the BSE Hamiltonian. For h -BN the same \mathbf{k} -mesh and 80 unoccupied states were sufficient to capture the absorption fine structure.

For comparison with experiment, a Gaussian broadening of 0.2 eV full width at half maximum is applied to the spectra, which are aligned at the π^* peak by a rigid energy shift of the DFT energies.

Results and discussion

To consider the effect of distortions on the absorption spectra, we first limit our study to the Γ point modes. We find that the E_{2g} and E_{1u} vibrations have the most significant effects on the spectra for both graphite and h -BN, and lead to very similar results. Other phonon modes show only smaller effects, in particular for out-of-plane movements of the atoms, as compared with the unperturbed lattice. The possible effect on the spectra can be recognized already from the respective unoccupied density of states for the cells. Both E_{2g} and E_{1u} modes change the in-plane bond lengths as evident from the eigenvectors shown in the inset of Fig. 1. The calculated BSE spectra for different vibrational amplitudes between 0.01 to 0.05 Å, along the E_{2g} phonon mode are shown in Fig. 1. The first σ^* peak is found to shift almost proportional to δ . Most important, the σ^* peak clearly splits into two, already at a displacement of 0.02 Å. To demonstrate, that this is indeed important at temperatures where experimental spectra are typically recorded, we have computed the root mean square

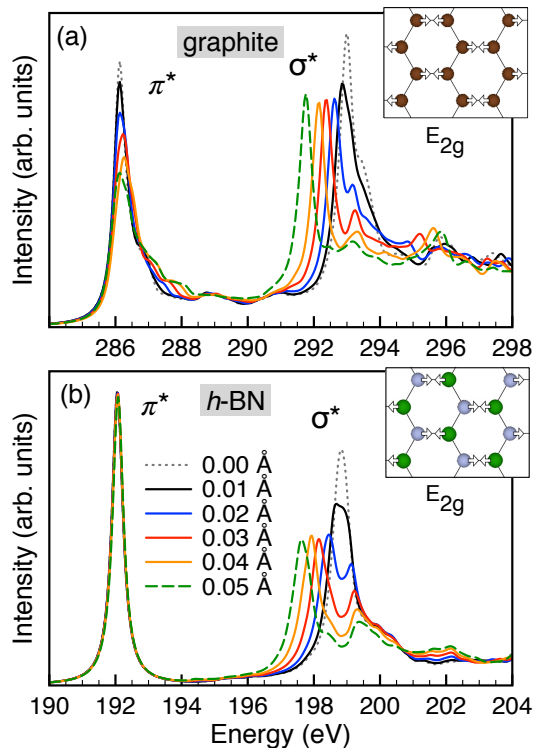


Figure 1: Calculated core-level spectra from the solution of the BSE for a) graphite and b) h -BN, accounting for different displacements $\delta = 0.01$ to 0.05 Å according to the E_{2g} phonon mode. The insets show the corresponding displacement patterns.

atomic displacement, δ_{rms} , as a function of temperature for the E_{2g} and E_{1u} phonon modes. We find that zero-point vibrations are dominating up to ~ 500 K owing to the high phonon frequency modes of 47.4 THz for graphite and 40.2 THz for h -BN (not shown). Without considering anharmonic effects, δ_{rms} is around 0.03 Å at RT and below. Only at extremely high temperatures, the quantum-mechanical displacement converges to the classical limit. The great sensitivity of the spectra to atomic vibrations, already present by zero-point motion, also holds true for h -BN.

In Fig. 2 we show the single excitations contributing to the σ^* and π^* peak structures as obtained from the BSE calculations for the equilibrium geometry (black lines) and displacements according to the E_{2g} phonon modes with $\delta = 0.03$ Å (red lines) for both materials. Many excitations with low oscillator strength between the π^* and σ^* peaks can be seen for graphite, but not for h -BN π^* . At the equilibrium structure, the core-edge in graphite con-

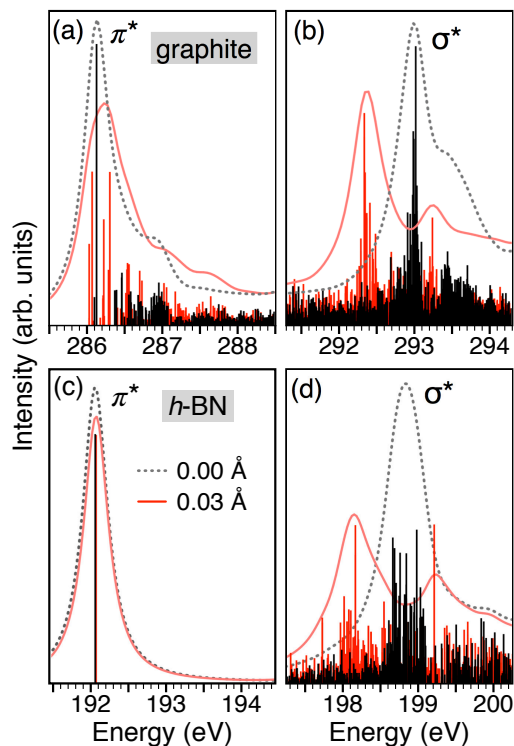


Figure 2: Relative oscillator strengths for the excitations contributing to the a) π^* and b) σ^* peak for the C K -edge in graphite and for the c) π^* and d) σ^* peak for the B K -edge in h -BN. Black lines correspond to the equilibrium positions and red lines to a displacement of $\delta = 0.03 \text{ \AA}$ in the E_{2g} mode. The broadened spectra are indicated by dashed black lines.

sists of two strongly bound core excitons. More complicated excitonic features are found for the displaced geometries, characterized by an increasing number of excitations and redistribution of oscillator strength. In h -BN, the π^* core-edge consists of a single strongly bound core exciton, which is practically not affected by the symmetry-breaking in-plane modes. Here also a slightly more strongly bound core exciton exists, but it has vanishing oscillator strength due to its s -orbital character. For both systems, the σ^* -region can be described as a mixture of different excitations, whose main features are several strongly bound core excitons with high oscillator strengths. In particular, the σ_2^* structure in h -BN appears as mainly due to a strong single excitation, while several excitations are observed for graphite.

In Fig. 3, we compare the calculated BSE results, i.e. the room temperature (RT) average (dark blue lines) – further discussed below, the ones representing an E_{2g} vibration with $\delta =$

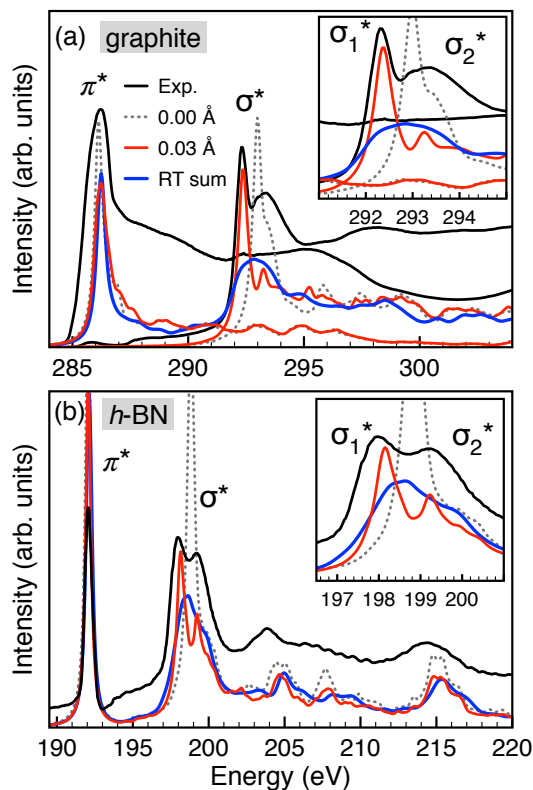


Figure 3: Experimental XANES (black full lines) and calculated BSE spectra for a) the carbon K -edge in graphite and b) the B K -edge in h -BN for the equilibrium geometry (gray dotted lines), the RT average (dark blue lines) and for displacements of $\delta = 0.03 \text{ \AA}$ (red lines) according to the E_{2g} phonon mode.

0.03 \AA (red lines), as well as the one for the equilibrium structure (gray dotted lines), with the experimental XANES spectra (black lines). For graphite, the respective out-of-plane and in-plane contributions are shown separately. The experimental spectra were obtained for a highly oriented pyrolytic graphite (HOPG) sample of high purity manufactured by chemical vapor deposition (CVD) and cleaved to obtain a fresh surface. The measurement was performed at 300 K and $\sim 1 \times 10^{-7} \text{ Pa}$ at the undulator beamline I511-3 on the MAX II ring of the MAX IV Laboratory (Lund University, Sweden).³³ The energy resolution at the C 1s edge of the beamline monochromator was 0.1 eV. The spectra were recorded at 15° (along the c -axis, near perpendicular to the basal ab plane) and 90° (normal, parallel to the basal ab -plane) incidence angles and normalized by the step edge below and far above the absorption thresholds. The experimental data for the B K -edge in h -BN are taken from

1
2
3 Ref.³⁴
4

5 We recall here, that the upper part of the X-ray absorption spectrum of graphite has so
6 far been ambiguously interpreted, partly owing to the fact that first-principles studies^{10–13}
7 could not reproduce the σ_2^* peak. The feature was early on interpreted as due to vibronic
8 coupling by Ma *et al.*,⁸ arguing for strong vibrational effects in diamond and graphite based
9 on X-ray emission spectra. Symmetry breaking by vibrations in graphite was put forward by
10 Harada *et al.* by model calculations of resonant X-ray emission.^{20–22} In contrast, Brühwiler
11 *et al.* interpreted σ_1^* as an excitonic feature, in line with Ref.,⁸ and σ_2^* as a delocalized band-
12 like contribution.³⁵ Also, delocalized sp^2 orbitals without influence of the core-hole, i.e., an
13 initial-state effect, was suggested¹³ as its origin.
14
15
16
17
18
19
20
21
22

23 For both materials, we find that including the effect of the in-plane phonon modes at the
24 Γ point, as seen in Fig. 3, essentially reproduce the double peak structures corresponding to
25 the σ^* peak observed in experiment. In the case of graphite, there is an effective widening of
26 the σ^* peak region into the measured fine structure with the σ_1^* and σ_2^* peaks.^{8,9} A similar
27 trend is observed for the B *K*-edge in *h*-BN, reproducing the characteristic camel-back like
28 feature.³⁴ A difference between these theoretical results of the two systems including the
29 lattice distortion effect, is that the intensity and the shape of the π^* peak display virtually
30 no change in *h*-BN, as opposite to graphite.
31
32
33
34
35
36
37
38

39 We consider the spectra at room temperature (RT) by sampling over the canonical en-
40 semble as described in the Methodology section. The result of the corresponding BSE cal-
41 culations are shown in Fig. 4 with individual spectra for the supercells (light blue lines)
42 compared with the average sum at RT (dark blue lines) and equilibrium (gray dotted lines).
43 It is clear that the σ^* -region is significantly affected with a shift towards lower energy and
44 a redistribution of intensity. In the case of graphite the sharp peak is much reduced into
45 a broadened shape, while *h*-BN shows features closer to a double-peak structure. On the
46 other hand, the positions of the π^* peaks are almost the same, although with a slight ef-
47 fect at the C *K*-edge. In general, the effect of the averaging process is a reduction of the
48
49
50
51
52
53
54
55
56
57
58
59
60

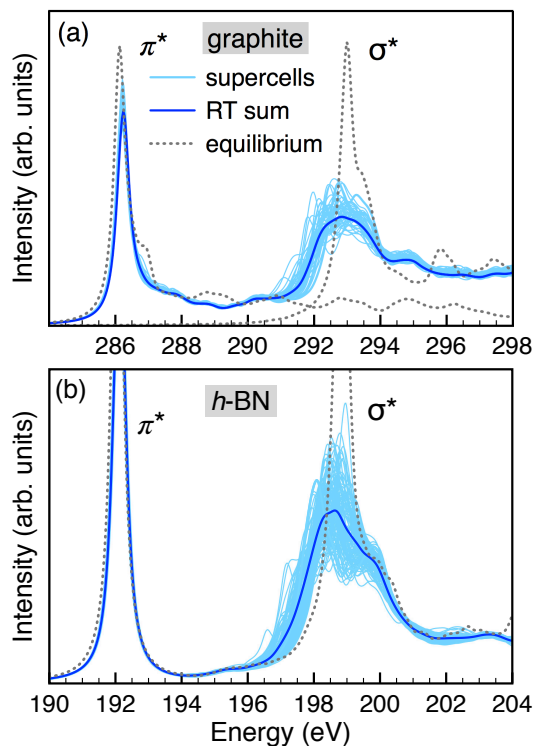


Figure 4: Calculated core-level spectra from the solution of the BSE for a) graphite and b) *h*-BN, with results from the set of selected supercells (light blue lines) and the corresponding RT average (dark blue lines). For comparison, the spectra of the equilibrium structure is shown (gray dotted lines).

dominant spectral features, originating from the in-plane phonon modes, as observed before. It remains unresolved though why these modes play a dominant role as one may conclude from the comparison with experiment. This observation points towards other mechanisms at play, e.g. core-hole life time effects, which are not included in the present modeling.

Conclusions

In summary, we have demonstrated the importance of including vibrational effects for XANES/ELNES spectra of the C *K*-edge in graphite and B *K*-edge in *h*-BN. We anticipate that zero-point motions and lattice symmetry breaking can be important for many other materials. Graphite and hexagonal boron nitride are archetypical layered structures, which share many features with the related 2D materials of graphene and BN monolayers. Thus

1
2
3 we expect similar behavior also in these systems. Generally, we point to low-dimensional
4 structures, where electron-phonon coupling is typically enhanced, and particularly to mate-
5 rials with light atoms, that exhibit high vibrational frequencies. Since we expect vibrational
6 effects to be visible in a large temperature range, we encourage new temperature-dependent
7 experiments on light-weight low-dimensional materials.
8
9
10
11
12

13 14 15 **Acknowledgement**

16
17
18 J.J. Rehr is acknowledged for providing access to the OCEAN program,³⁶ used for comparative
19 tests. W.O. acknowledges support from the Swedish Government Strategic Research Area
20 in Materials Science on Functional Materials at Linköping University (Faculty Grant SFO-
21 Mat-LiU no. 2009 00971) and Knut and Alice Wallenbergs Foundation project Strong Field
22 Physics and New States of Matter CoTXS (2014-2019). We would like to thank the staff at
23 MAX-IV Laboratory for experimental support and Dr. Atsushi Togo for valuable discussions
24 on theory. M.M. acknowledges financial support from the Swedish Energy Research (no.
25 43606-1) and the Carl Trygger Foundation (CTS16:303, CTS14:310). The calculations were
26 carried out at the National Supercomputer Centre (NSC) at Linköping University, supported
27 by SNIC. Support for I.T. by JSPS KAKENHI 26630295 and 25106005, T.M. by JSPS
28 KAKENHI 26249092, and C.D. by the Deutsche Forschungsgemeinschaft through SFB 658
29 and SFB 951, are acknowledged.
30
31
32
33
34
35
36
37
38
39
40
41
42
43
44

45 **References**

- 46
47
48 (1) Mizoguchi, T.; Olovsson, W.; Ikeno, H.; Tanaka, I. Theoretical ELNES using One-
49 Particle and Multi-Particle Calculations. *Micron* **2010**, *41*, 695-709.
50
51
52
53 (2) Kohn, W. Nobel Lecture: Electronic Structure of Matter-Wave Functions and Density
54 Functionals. *Rev. Mod. Phys.* **1999**, *71*, 1253-1266.
55
56
57
58
59
60

- 1
2
3 (3) Hébert, C. Practical Aspects of Running the WIEN2k Code for Electron Spectroscopy.
4 *Micron* **2007**, *38*, 12-28.
5
6
7
8 (4) Tanaka, I.; Mizoguchi, T.; Yamamoto, T. XANES and ELNES in Ceramic Science. *J.*
9 *Am. Ceram. Soc.* **2005**, *88*, 2013-2029.
10
11
12 (5) Olovsson, W.; Tanaka, I.; Mizoguchi, T.; Puschnig, P.; Ambrosch-Draxl, C. All-
13 electron Bethe-Salpeter Calculations for Shallow-Core X-Ray Absorption Near-Edge
14 Structures. *Phys. Rev. B: Condens. Matter Mater. Phys.* **2009**, *79*, 041102R.
15
16
17 (6) Olovsson, W.; Tanaka, I.; Puschnig, P.; Ambrosch-Draxl, C. Near-Edge Structures
18 from First Principles All-Electron Bethe-Salpeter Equation Calculations. *J. Phys.:
19 Condens. Matter* **2009**, *21*,104205.
20
21
22 (7) Olovsson, W.; Tanaka, I.; Mizoguchi, T.; Radtke, G.; Puschnig, P.; Ambrosch-Draxl,
23 C. Al L_{2,3} Edge X-Ray Absorption Spectra in III-V Semiconductors: Many-Body
24 Perturbation Theory in Comparison with Experiment. *Phys. Rev. B: Condens. Matter
25 Mater. Phys.* **2011**, *83*, 195206.
26
27
28 (8) Ma, Y.; Skytt, P.; Wassdahl, N.; Glans, P.; Mancini, D.C.; Guo, J.; Nordgren, J. Core
29 Excitons and Vibronic Coupling in Diamond and Graphite. *Phys. Rev. Lett.* **1993**,
30 *71*, 3725-3728.
31
32
33 (9) Moscovici, J.; Loupiaz, G.; Parent, Ph.; Tourillon, G. Polarization-Dependent Boron
34 and Nitrogen K NEXAFS of Hexagonal BN. *J. Phys. Chem. Solids* **1996**, *57*, 1159-
35 1161.
36
37
38 (10) Shirley, E.L. Ab Initio Inclusion of Electron-Hole Attraction: Application to X-Ray
39 Absorption and Resonant Inelastic X-Ray Scattering. *Phys. Rev. Lett.* **1998**, *80*, 794-
40 797.
41
42
43
44
45
46
47
48
49
50
51
52
53
54
55
56
57
58
59
60

- 1
2
3 (11) Ahuja, R.; Brühwiler, P.A.; Wills, J.M.; Johansson, B.; Mårtensson, N.; Eriksson,
4 O. Theoretical and Experimental Study of the Graphite 1s X-Ray Absorption Edges.
5 *Phys. Rev. B: Condens. Matter Mater. Phys.* **1996**, *54*, 14396-14404.
6
7
8
9
10 (12) Moreau, P.; Boucher, F.; Goglio, G.; Foy, D.; Mauchamp, V.; Ouvrard, G. Electron
11 Energy-Loss Spectra Calculations and Experiments as a Tool for the Identification of
12 a Lamellar C₃N₄ Compound. *Phys. Rev. B: Condens. Matter Mater. Phys.* **2006**, *73*,
13 195111.
14
15
16
17
18 (13) Wessely, O.; Katsnelson M.I.; Eriksson, O. Ab Initio Theory of Dynamical Core-Hole
19 Screening in Graphite from X-Ray Absorption Spectra. *Phys. Rev. Lett.* **2005**, *94*,
20 167401.
21
22
23
24
25 (14) Tanaka, I.; Araki, H.; Yoshiya, M.; Mizoguchi, T.; Ogasawara, K.; Adachi, H. First-
26 Principles Calculations of Electron-Energy-Loss Near-Edge Structure and Near-Edge
27 X-Ray-Absorption Fine Structure of BN Polytypes using Model Clusters. *Phys. Rev.*
28 *B: Condens. Matter Mater. Phys.* **1999**, *60*, 4944.
29
30
31
32
33 (15) Carlisle, J.A.; Shirley, E.L.; Terminello, L.J.; Jia, J.J.; Callcott, T.A.; Ederer, D.L.;
34 Perera, R.C.C.; Himpsel, F.J. Band-Structure and Core-Hole Effects in Resonant In-
35 elastic Soft-X-Ray Scattering: Experiment and Theory *Phys. Rev. B: Condens. Matter*
36 *Mater. Phys.* **1999**, *59*, 7433.
37
38
39
40
41 (16) Tinte, S.; Shirley, E.L. Vibrational Effects on SrTiO₃ Ti 1s Absorption Spectra Studied
42 using First-Principles Methods. *J. Phys.: Condens. Matter* **2008**, *20*, 365221.
43
44
45
46 (17) Gilmore K.; Shirley, E.L. Numerical Quantification of the Vibronic Broadening of the
47 SrTiO₃ Ti L-Edge Spectrum. *J. Phys.: Condens. Matter* **2010**, *22*, 315901.
48
49
50
51 (18) Skytt, P.; Glans, P.; Mancini, D.C.; Guo, J.-H.; Wassdahl, N.; Nordgren, J.; Ma,
52 Y. Angle-Resolved Soft-X-ray Fluorescence and Absorption Study of Graphite. *Phys.*
53 *Rev. B: Condens. Matter Mater. Phys.* **1994**, *50*, 10457-10461.
54
55
56
57
58
59
60

- 1
2
3 (19) Batson, P.E. Carbon 1s Near-Edge-Absorption Fine Structure in Graphite. *Phys. Rev.*
4 *B: Condens. Matter Mater. Phys.* **1993**, *48*, 2608-2610.
5
6
7
8 (20) Harada, Y.; Tokushima, T.; Takata, Y.; Takeuchi, T.; Kitajima, Y.; Tanaka, S.;
9 Kayanuma, Y.; Shin, S. Dynamical Symmetry Breaking under Core Excitation in
10 Graphite: Polarization Correlation in Soft X-Ray Recombination Emission. *Phys. Rev.*
11 *Lett.* **2004**, *93*, 017401.
12
13
14
15
16
17 (21) Tanaka, S.; Kayanuma, Y. Dynamics in Resonant X-Ray Emission of the Core Exciton
18 State: Competition between Electron Itinerancy and Lattice Relaxation. *Phys. Rev.*
19 *B: Condens. Matter Mater. Phys.* **2005**, *71*, 024302.
20
21
22
23
24 (22) Yasui, A.; Kayanuma, Y.; Tanaka, S.; Harada, Y. Dynamical Changeover of Core
25 Exciton State of Graphite and Resonant X-Ray Emission Spectrum: From Shallow to
26 Deep Level with Symmetry Breaking. *Phys. Rev. B: Condens. Matter Mater. Phys.*
27 **2006**, *74*, 205404.
28
29
30
31
32 (23) Marini, A. Ab Initio Finite-Temperature Excitons. *Phys. Rev. Lett.* **2008**, *101*, 106405.
33
34
35 (24) Patrick C.E.; Giustino, F. Quantum Nuclear Dynamics in the Photophysics of Dia-
36 mondoids. *Nat. Commun.* **2013**, *4*, 2006.
37
38
39
40 (25) Nemausat, R.; Cabaret, D.; Gervais, C.; Brouder, C.; Trcera, N.; Bordage, A.; Errea,
41 I.; Mauri, F. Phonon Effects on X-Ray Absorption and Nuclear Magnetic Resonance
42 Spectroscopies. *Phys. Rev. B: Condens. Matter Mater. Phys.* **2015**, *92*, 144310.
43
44
45
46
47 (26) Vinson, J.; Jach, T.; Müller, M.; Unterumsberger, R.; Beckhoff, B. Resonant X-Ray
48 Emission of Hexagonal Boron Nitride. *Phys. Rev. B: Condens. Matter Mater. Phys.*
49 **2017**, *96*, 205116.
50
51
52
53 (27) Shulumba, N.; Hellman, O.; Minnich, A.J. Intrinsic Localized Mode and Low Thermal
54 Conductivity of PbSe. *Phys. Rev. B: Condens. Matter Mater. Phys.* **2017**, *95*, 014302.
55
56
57
58
59
60

- 1
2
3 (28) Shulumba, N.; Hellman, O.; Minnich, A.J. Lattice Thermal Conductivity of Polyethy-
4 lene Molecular Crystals from First-Principles Including Nuclear Quantum Effects.
5 *Phys. Rev. Lett.* **2017**, *119*, 185901.
6
7
8
9
10 (29) Gulans, A.; Kontur, S.; Meisenbichler, C.; Nabok, D.; Pavone, P.; Rigamonti, S.;
11 Sagmeister, S.; Werner, U.; Draxl, C. Exciting: a Full-Potential All-Electron Package
12 Implementing Density-Functional Theory and Many-Body Perturbation Theory. *J.*
13 *Phys.: Condens. Matter* **2014**, *26*, 363202.
14
15
16
17
18 (30) Sagmeister, S.; Ambrosch-Draxl, C. Time-Dependent Density Functional Theory Ver-
19 sus Bethe-Salpeter Equation: an All-Electron Study. *Phys. Chem. Chem. Phys.* **2009**,
20 *11*, 4451-4457.
21
22
23
24
25 (31) Olovsson, W.; Weinhardt, L.; Fuchs, O.; Tanaka, I.; Puschnig, P.; Umbach, E.; Heske,
26 C.; Draxl, C. The Be K-edge in Beryllium Oxide and Chalcogenides: Soft X-Ray
27 Absorption Spectra from First-Principles Theory and Experiment. *J. Phys.: Condens.*
28 *Matter* **2013**, *25*, 315501.
29
30
31
32
33 (32) Perdew, J. P.; Burke, K.; Ernzerhof, M. Generalized Gradient Approximation Made
34 Simple. *Phys. Rev. Lett.* **1996**, *77*, 3865-3868.
35
36
37
38
39 (33) Magnuson, M.; Andersson, M.; Lu, J.; Hultman, L.; Jansson, U. Electronic Struc-
40 ture and Chemical Bonding of Amorphous Chromium Carbide Thin Films. *J. Phys.:*
41 *Condens. Matter* **2012**, *24*, 225004.
42
43
44
45 (34) Li, D.; Bancroft, G.M.; Fleet, M.E. B K-edge XANES of Crystalline and Amorphous
46 Inorganic Materials. *J. Electron Spectrosc. Relat. Phenom.* **1996**, *79*, 71-73.
47
48
49
50 (35) Brühwiler, P.A.; Maxwell, A.J.; Puglia, C.; Nilsson, A.; Andersson, S.; Mårtensson,
51 N. π^* and σ^* Excitons in C 1s Absorption of Graphite *Phys. Rev. Lett.* **1995**, *74*,
52 614-617.
53
54
55
56
57
58
59
60

- 1
2
3 (36) Gilmore, K.; Vinson, J.; Shirley, E.L.; Pendergast, D.; Pemmaraju, C.D.; Kas, J.J.;
4
5 Vila, F.D.; Rehr, J.J. Efficient Implementation of Core-Excitation Bethe-Salpeter
6
7 Equation Calculations. *Computer Physics Communications* **2015**, *197*, 109-117.
8
9
10
11
12
13
14
15
16
17
18
19
20
21
22
23
24
25
26
27
28
29
30
31
32
33
34
35
36
37
38
39
40
41
42
43
44
45
46
47
48
49
50
51
52
53
54
55
56
57
58
59
60

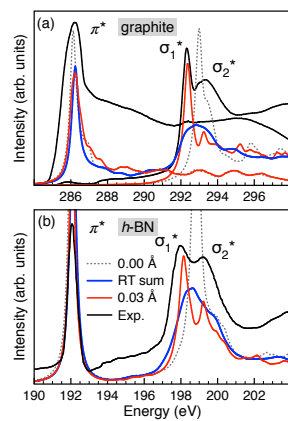


Figure 5: TOC graphics